Abdominal Radiology (2019) 44:2921–2928
https://doi.org/10.1007/s00261-019-02014-2

TECHNICAL

Automated segmentation and quantification of aortic calcification at abdominal CT: application of a deep learning-based algorithm to a longitudinal screening cohort

Peter M. Graffy[1] · Jiamin Liu[2] · Stacy O'Connor[3] · Ronald M. Summers[2] · Perry J. Pickhardt[1]

Published online: 11 April 2019

Abstract

Objective To investigate an automated aortic calcium segmentation and scoring tool at abdominal CT in an adult screening cohort.

Methods Using instance segmentation with convolutional neural networks (Mask R-CNN), a fully automated vascular calcification algorithm was applied to a data set of 9914 non-contrast CT scans from 9032 consecutive asymptomatic adults (mean age, 57.5 ± 7.8 years; 4467 M/5447F) undergoing colonography screening. Follow-up scans were performed in a subset of 866 individuals (mean interval, 5.4 years). Automated abdominal aortic calcium volume, mass, and Agatston score were assessed. In addition, comparison was made with a separate validated semi-automated approach in a subset of 812 cases.

Results Mean values were significantly higher in males for Agatston score (924.2 ± 2066.2 vs. 564.2 ± 1484.2, $p < 0.001$), aortic calcium mass (222.2 ± 526.0 mg vs. 144.5 ± 405.4 mg, $p < 0.001$) and volume (699.4 ± 1552.4 ml vs. 426.9 ± 1115.5 HU, $p < 0.001$). Overall age-specific Agatston scores increased an average of 10%/year for the entire cohort; males had a larger Agatston score increase between the ages of 40 to 60 than females (91.2% vs. 75.1%, $p < 0.001$) and had significantly higher mean Agatston scores between ages 50 and 80 ($p < 0.001$). For the 812-scan subset with both automated and semi-automated methods, median difference in Agatston score was 66.4 with an r^2 agreement value of 0.84. Among the 866-patient cohort with longitudinal follow-up, the average Agatston score change was 524.1 ± 1317.5 (median 130.9), reflecting a mean increase of 25.5% (median 73.6%).

Conclusion This robust, fully automated abdominal aortic calcification scoring tool allows for both individualized and population-based assessment. Such data could be automatically derived at non-contrast abdominal CT, regardless of the study indication, allowing for opportunistic assessment of cardiovascular risk.

Keywords Aortic calcium · Deep learning · Fully automated · Artificial intelligence · Cardiovascular disease

Abbreviations

R-CNN	Convolutional neural networks
CVD	Cardiovascular disease
CT	Computed tomography
ROI	Region of interest
HU	Hounsfield unit

Introduction

Cardiovascular disease (CVD) is the leading cause of mortality in the US and remains one of the greatest public health concerns of our time. CVD currently affects an estimated 92.1 million Americans, and the American Heart Association expects nearly 44% of the US population to have some form of heart disease by 2030 [1, 2]. Many clinical methods have been developed to assess the risk factors of CVD, including the Framingham Risk Score [3], lipid screening [4], hypertension management [5], as well as imaging techniques that measure atherosclerosis and calcium aggregation

✉ Perry J. Pickhardt
ppickhardt2@uwhealth.org

[1] E3/311 Clinical Science Center, University of Wisconsin School of Medicine and Public Health, 600 Highland Ave., Madison, WI 53792-3252, USA

[2] Radiology & Imaging Sciences, National Institutes of Health Clinical Center, Bethesda, MD, USA

[3] Department of Radiology, Medical College of Wisconsin, Milwaukee, WI, USA

[6–10]. Though utilized less frequently than other clinical techniques due to cost and accessibility, imaging modalities such as computed tomography (CT) have shown to be robust tools at characterizing CVD and its associated comorbidities [11–14].

CT imaging is generally considered the most effective technique to characterize aortic calcification in adults. Though calcification can be assessed by either dual energy X-ray absorptiometry or non-contrast CT, the latter offers the distinct advantage of quantifying the extent of mural calcium in the aorta [6, 7, 15]. Manual, semi-automated, and automated methods have been developed for CT to accurately detect and score aortic calcification at both the patient and population levels [12, 16, 17]. Furthermore, deep-learning-based algorithms that detect and compute aortic calcification have the potential to be a valuable clinical asset when applied to both individual patient scans and more broadly to adult screening populations. Few studies have investigated the utilization of a fully automated approach to characterize abdominal aortic calcification at the population level, including changes over time. The purpose of this study was to apply an automated CT-based abdominal aortic calcium segmentation algorithm to a large asymptomatic adult cohort undergoing low-dose non-contrast abdominal CT to determine normal age- and gender-related differences at the population level.

Materials and methods

Patient population

This was an IRB-approved, HIPAA-compliant retrospective cohort study. 9032 consecutive adults underwent initial low-dose non-contrast abdominal CT for colonography screening at a single academic medical center between April 2004 and December 2016. 9930 studies were initially considered for inclusion, with 16 excluded based on algorithmic segmentation failures, yielding a total of 9914 eligible studies which served as the primary cohort. 882 patients had at least one follow-up CTC study, which was included to assess for longitudinal changes over time. A subset of 812 consecutive patients were also evaluated with a validated semi-automated technique. All patient information was anonymized prior to investigation.

CT scanning protocol

Specifics relating to CT colonography technique such as bowel preparation and distention have been previously described and are beyond the scope or concern of this study [18]. Breath-hold CT acquisition of the abdomen and pelvis without IV contrast was obtained in both supine and prone positions, but only the former was utilized herein for abdominal aortic calcium assessment. All CT scans were performed on 8–64 multi-detector-row scanners (GE Healthcare). Scanning was performed at 120 kV with reduced-dose mA settings (typically modulated between 30 and 300). Axial images for extracolonic evaluation reconstructed using 5 mm slice thickness at 3 mm intervals were utilized for our study.

Algorithms for abdominal aortic calcium measurements

The atherosclerotic plaque detection and segmentation algorithm utilized in this study represents a fully automated deep-learning system developed and trained at our institution on a separate low-dose CT cohort [19–21]. Specifically, the system was primarily trained on an independent training dataset of 112 low-dose CT scans from a different institution, consisting of over 4500 aortic plaques [19].

The CT images are first processed by fully automated spine segmentation and labeling software that identifies the slice that corresponds to the superior and inferior endplates of each vertebral body from T12 to L5 [22]. Then, a semi-supervised learning method with Mask R-CNN was utilized for automated detection and segmentation of atherosclerotic plaques, due to its precise and rapid segmentation [23]. Mask R-CNN extends Faster R-CNN [22] with a segmentation branch to generate masks with different classes. It employs a single-stage training process to jointly detect, classify, and segment plaques. In this study, a first Mask R-CNN with ResNet50 is initialized with COCO pre-trained model and fine-tuned with the supervisedly labeled plaques. For hard negative mining, false positives with high prediction scores are unsupervisedly clustered by k-means. A second Mask R-CNN is retrained by fine-tuning the first Mask R-CNN model with the plaques and clustered false positives. To further reduce false-positive plaque detections, the system analyzes both axial and sagittal CT image volumes. Plaque detections are retained for voxels detected on both the axial and sagittal image volumes, and can be viewed image-by-image for confirmation. A schematic example of the visual appearance of this segmentation and quantification is shown in (Fig. 1).

Atherosclerotic plaque quantification is performed by calculating the Agatston, volume, and mass scores of each plaque according to published methods [24]. The scores for each slice from the superior endplate of L1 through the middle of L4 were summed to create a per-patient score. Note that the scores can be much higher than those typically encountered in the coronary arteries due to the greater diameter and length of the abdominal aorta.

The atherosclerotic plaque detection, segmentation and measurement algorithm takes about 6 min to process an

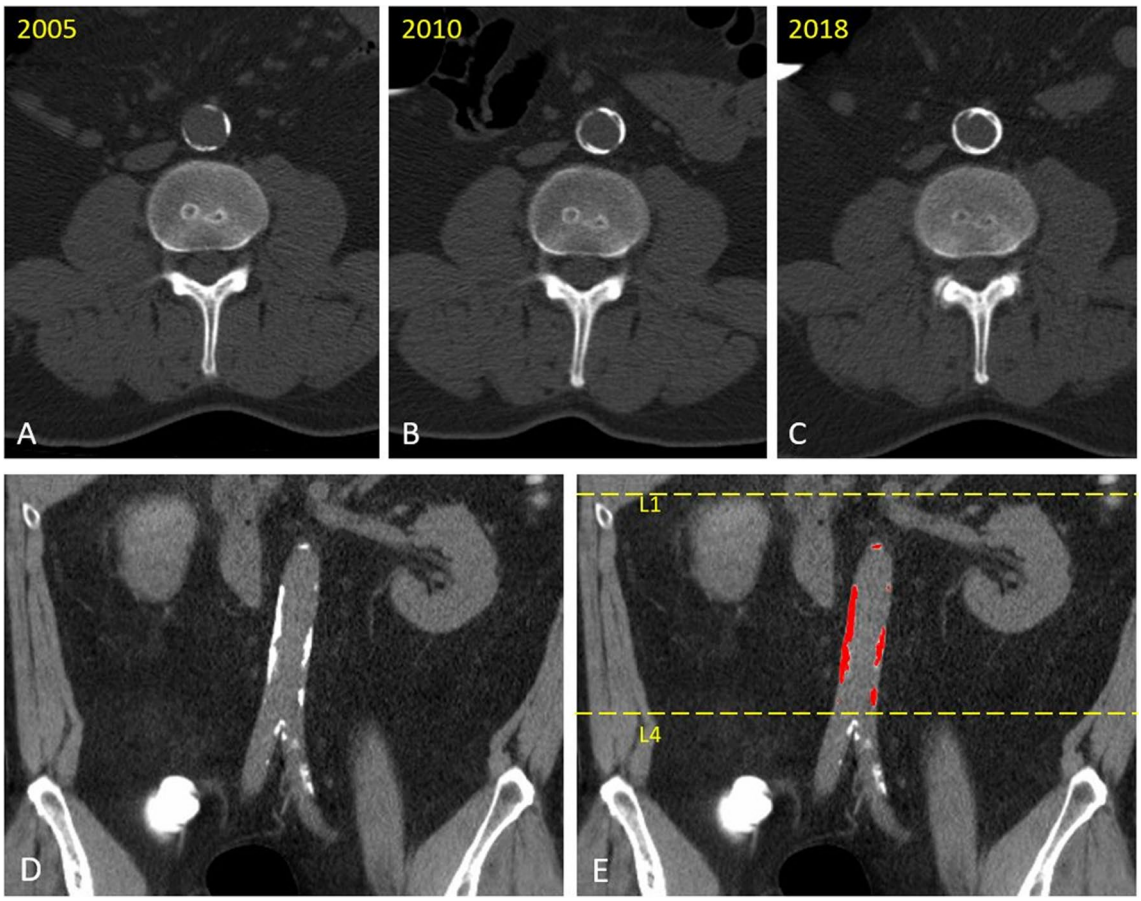

Fig. 1 Non-contrast CT images of the abdominal aorta over time in 57-year-old man (at time of initial CT) for schematic depiction of the automated calcium tool segmentation. **a**–**c** Transverse (axial) images at the L3 level show progressive increase in abdominal aortic calcification over a 13-year interval. **d** and **e** Coronal image without (**d**) and with (**e**) schematic overlays depict the prescribed L1–L4 level (between the dotted lines) localized by the automated tool, as well as the segmented aortic calcification (red areas) for quantification. In practice, the automatically segmented plaques can be quickly reviewed on an image-by-image basis

abdominal study (2.4 GHz Intel E5-2680v4, NVIDIA K80 GPU and 8 GB memory per CPU).

For comparison with this fully automated method, we utilized abdominal aortic calcium results in a subset of 812 patients that were previously obtained using a validated semi-automated coronary calcium screening tool applied to the abdominal aorta (V3D-Calcium Scoring; Viatronix) [17]. Of note, this semi-automated univariate method has been shown to be more predictive of future cardiovascular events than the multivariate Framingham risk score (FRS) [17]. This semi-automated method consisted of direct manual ROI segmentation of the abdominal aorta, which differs from the vertebral level method for the automated technique. A Hounsfield unit (HU)-based region-growing algorithm (threshold set at 130 HU) captured the calcium load, which was reported as volume, mass, and Agatston score. For the purposes of comparison with the automated method in this study, we considered only the semi-automated Agatston scores.

Statistical analysis

Summary statistics were collected for the patient population based on age and gender. In patients with follow-up CT scans, changes in Agatston score, volume, and mass were recorded, as was annual change, which was derived by dividing by the time interval between initial and follow-up CT for each patient. Percent change was calculated by taking the difference between the two scans, dividing by the initial value, and multiplying by 100. Percent change over time was calculated by taking the percent change and dividing by the time interval between scans. Comparison of means was done using independent t tests between genders and ages with a null hypothesis value of 0.05. Data processing and analysis were performed using base R (R Core Team, v. 3.4.2).

Results

The mean age (± SD) of the 9032 individual patients included in this study was 57.5 ± 7.8 years (range 23–95); there were 4011 men and 5021 women. 866 patients (445 men and 421 women) underwent a follow-up study (mean interval, 5.4 years). Of the 812 patients evaluated by both automated and semi-automated techniques, 369 were male and 443 were female. Exclusions ($n = 16$) were primarily due to algorithmic failure to accurately determine the vertebral level, resulting in an overall failure rate of 0.2% (16/9930).

Aortic volume, mass, and Agatston score all showed non-normal population distributions irrespective of age or gender, with skew towards higher values (Fig. 2). Strong age-related increases were seen in the patient cohort for Agatston score, calcium volume, and mass (Fig. 3a). When separated by sex, mean male Agatston score was greater than that of females for every age category above the age of 40 (Fig. 3b). Mean values were also significantly higher in males for Agatston score (924.2 ± 2066.2 vs. 564.2 ± 1484.2, $p < 0.001$), aortic calcium mass (222.2 ± 526.0 mg vs. 144.5 ± 405.4 mg, $p < 0.001$) and volume (699.4 ± 1552.4 ml vs. 426.9 ± 1115.5 HU, $p < 0.001$). A total of 3054 adults (30.8%) had an Agatston score of zero, 5309 (53.6%) had a score < 100, 6641 (67.0%) had a score < 300, and 3273 (33.0%) had a score > 300.

Population-based data according to age and gender are shown in Table 1. Overall age-specific Agatston scores were higher by age an average of 10%/year; males had a larger Agatston score increase between the ages of 40 to 60 than females (91.2% vs. 75.1%, $p < 0.001$) and had significantly higher mean Agatston scores between ages 50 and 80 ($p < 0.001$) (Table 1). When compared with patient BMI, Agatston score showed nearly no association with an r^2 correlation coefficient of 0.0031. However, patients with a reported BMI of ≥ 30 had a mean Agatston score of 845.7 versus 649.3 for those with a BMI ≤ 29 ($p < 0.001$).

For the patient subset evaluated with both semi-automated and automated techniques, Agatston scores showed an r^2 correlation coefficient of 0.84, and the median difference in Agatston score was 66.4 (mean difference, 383.6). Bland–Altman analysis is shown in Fig. 4. Among the patient subset with longitudinal follow-up, the average

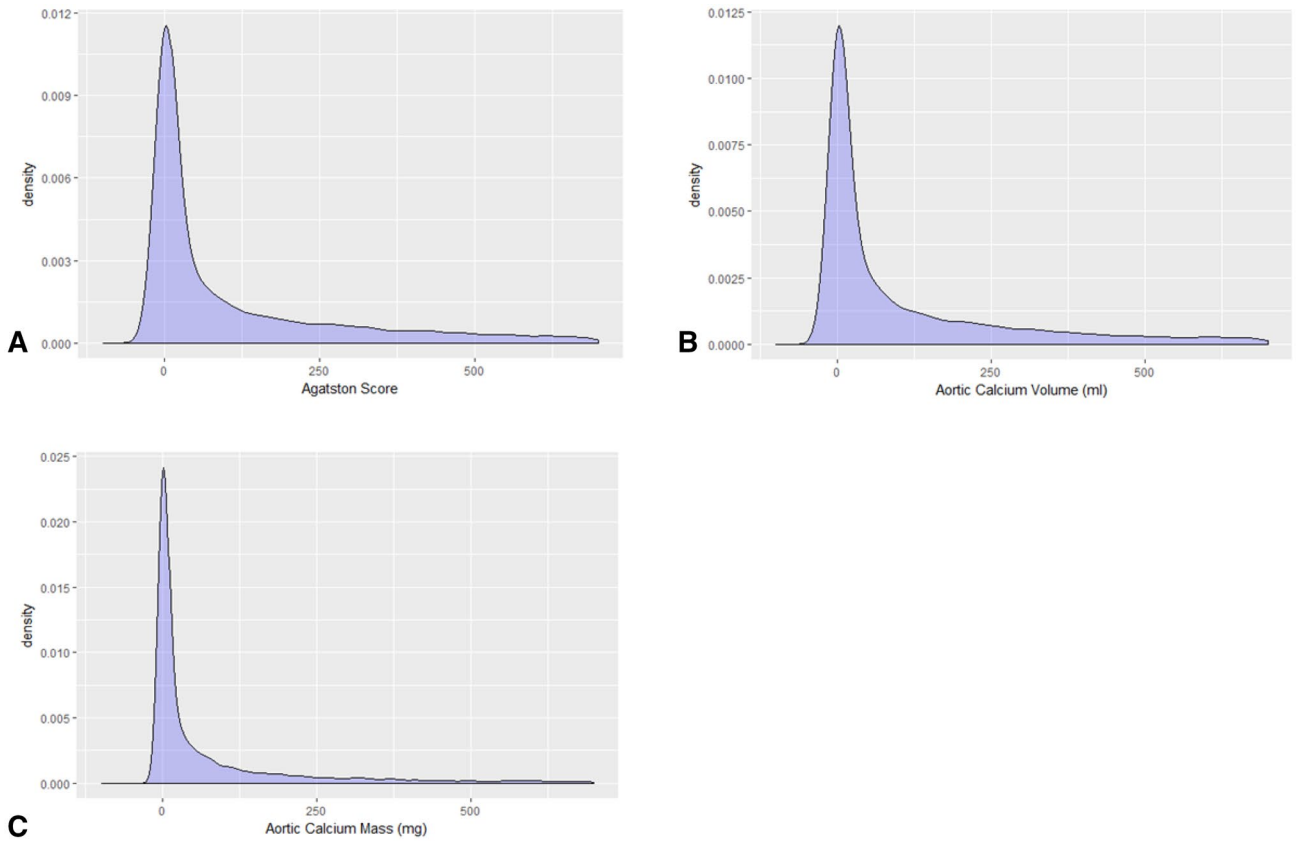

Fig. 2 Population density plot for automated abdominal aortic Agatston score (**a**), calcium volume (**b**), and calcium mass (**c**) for the entire study cohort. Note relatively normal peak near zero, but long tail skewing towards higher calcium loads

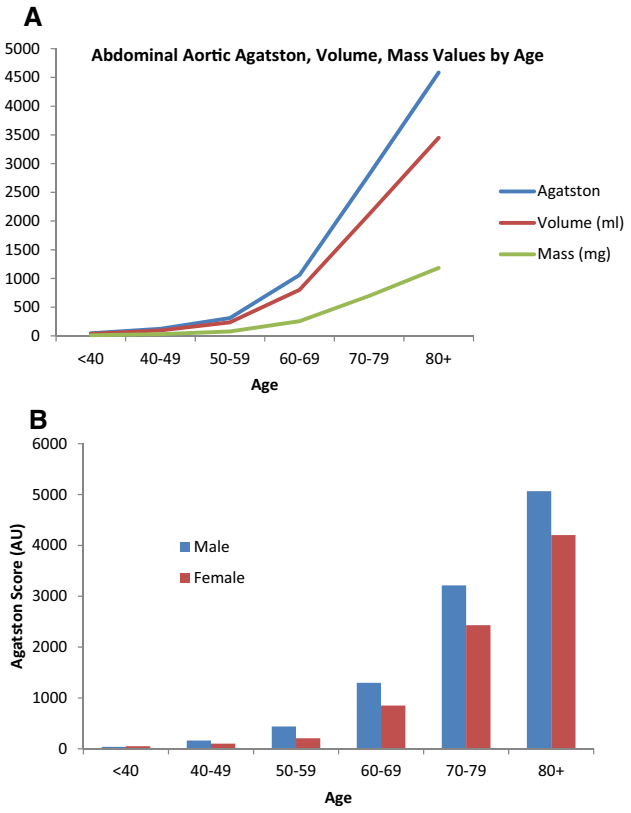

Fig. 3 Abdominal aortic calcium scores according to age and gender. **a** Plot of mean abdominal aortic Agatston scores, calcium volume, and calcium mass according to age. **b** Graph showing mean Agatston scores according to age and gender

Agatston score change was 524.1 ± 1317.5 (median, 130.9), reflecting a mean percent increase of 25.5% (median, 73.6%). The mean male Agatston change was 618.7 (13% from baseline) while the mean female change was 424.0 (39% from baseline).

Discussion

Given our relatively unique abdominal CT cohort of asymptomatic outpatient adults, our study provides useful normative values for abdominal aortic calcium levels, including age- and gender-related differences. In addition, we demonstrate the potential utility of the fully automated abdominal aortic calcification algorithm that we employed. To our knowledge, this retrospective cohort study is the first to achieve fully automated abdominal aortic calcium measurements on a large-asymptomatic screening population. With the information and CT tool provided by this study, clinicians and researchers can potentially assess for cardiovascular risk in adults on non-contrast abdominal CT scans, either

Table 1 Age- and gender-specific values for automated abdominal aortic calcification

Age	Male ($n=4467$)				Female ($n=5447$)				*p* value		
	n	Agatston	Volume (ml)	Mass (mg)	*n*	Agatston	Volume (ml)	Mass (mg)	Agatston	Volume	Mass
< 40	24	38.8 (136.9)	29.6 (103.3)	15.1 (62.2)	30	51.7 (210.7)	39.9 (158.4)	10.0 (35.7)	0.797	0.785	0.707
40–49	117	161.4 (373.1)	123.8 (282.8)	39.1 (95.1)	204	102.0 (365.9)	78.5 (278.1)	27.0 (106.3)	0.166	0.164	0.309
50–59	2740	439.2 (1076.4)	333.6 (809.9)	107.9 (284.6)	3421	207.7 (601.5)	158.1 (453.1)	52.9 (168.5)	0.001	0.001	0.001
60–69	1218	1298.6 (2141.6)	983.7 (1608.9)	305.8 (531.0)	1384	852.7 (1636.4)	645.7 (1231.0)	213.7 (430.0)	0.001	0.001	0.001
70–79	292	3213.5 (3922.1)	2422.7 (2942.0)	772.9 (1045.4)	313	2431.4 (2874.4)	1831.9 (2155.9)	626.8 (795.3)	0.005	0.005	0.053
80+	76	5066.3 (5213.2)	3810.4 (3908.4)	1235.7 (1329.3)	95	4202.6 (3960.0)	3159.9 (2968.0)	1141.0 (1197.0)	0.220	0.218	0.625

Numbers in parentheses are standard deviations

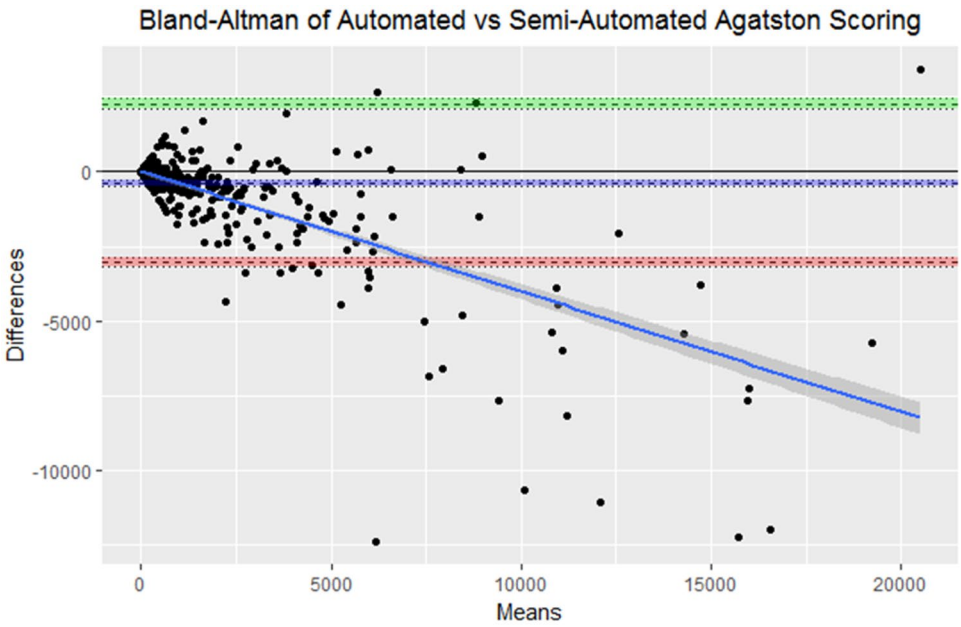

Fig. 4 Bland--Altman plot comparing Agatston scores for abdominal aortic calcification using automated and semi-automated techniques. The upper and lower limits of agreement were 2280.1 (95% CI 2120.1–2440.2) and − 3047.3 (95% CI − 2887 to − 3207) with a bias of − 383.6 (95% CI − 290 to − 477) toward the semi-automated measurement. Of note, the more discrepant scores involve patients with higher calcium loads, where classification is unlikely to be impacted

prospectively or retrospectively, performed for a variety of indications.

This study found mean Agatston scores to be significantly different for males and females within certain age ranges. On average, adult males had an approximately 33% greater Agatston score and calcium volume, and 27% more calcium mass than females. While both sexes gained abdominal aortic calcium (as measured by Agatston score) at about the same rate, males had significantly more calcium than females between the ages of 50 and 80. Furthermore, normative values for every age category were established for adult asymptomatic patients of both sexes between the ages of 40 and 80. Additionally, though CVD is related to obesity, and obesity is associated with both BMI and aortic calcium [25, 26], this study found no correlation between BMI and aortic calcium, which corresponds to the results found in other studies [27].

Various other studies have validated the efficacy of CT-based measurements of coronary artery calcification (CAC) or thoracic aortic calcification, typically using manual or semi-automated methods [28–30]. Agatston score is currently one of the most common measures to assess CVD risk at CT using Hounsfield Unit (HU) measurements to detect and quantify hard plaque accumulation. Many studies have employed a manual, automated, or semi-automated algorithms to simply detect the presence or absence of calcification or produce an Agatston score for patients with CAC [6, 7, 10–13]. Few studies have employed a fully automated method in a large-asymptomatic screening cohort to provide normative values for abdominal aortic calcium at CT. However, comparison with the previously validated semi-automated measurement method presented in this study [17] demonstrated the validity of the measurements obtained using this fully automated technique. A strong correlation was observed between the semi-automated and automated measurement techniques for the subset of patients who received both, despite the fact that the two techniques differed slightly in terms of anatomic segmentation. Cases with greater discrepancies tended to have a large calcium burden, such that the difference in scoring would likely have no clinical impact.

Abdominal CT is a commonly performed study on middle-age and older adults in the U.S. [31], which provides an opportunity to screen for multiple conditions beyond the study indication itself, such as osteoporosis, abdominal aortic aneurysm, hepatic steatosis, and metabolic syndrome [32–37]. If abdominal aortic calcium assessment is combined with other opportunistic screening tasks, such as bone mineral density, visceral fat, and muscle bulk, significant potential value may be added [17, 38–41]. These additional measures can be added without any additional time or dose to the patient, and with relatively little or no input from the radiologist. Going forward, we plan to investigate whether these automated measures are predictive of future adverse events, such as myocardial infarction, stroke, and death, among others. In a smaller cohort, semi-automated CT-based abdominal aortic calcification scoring was more predictive of future cardiovascular events than the Framingham risk score [17]. Ideally, risk profile screening for a wide variety of unsuspected conditions could help referring providers to initiate management plans for patients with concerning opportunistic screening results. Identification of such patients whose Agatston score drastically increases over time could be useful for studying the relationship between other

adverse health outcomes. Furthermore, we are not aware of studies to date that have established a relationship between changes in abdominal aortic calcium over time and adverse clinical outcomes, which is also something we plan to investigate further.

We acknowledge certain limitations to our study. All cases were derived from a single medical center employing scanners from a single CT vendor and non-contrast technique. Further external validation of the tool using a variety of different patient care settings and CT techniques is warranted. Testing and validation on contrast-enhanced CT scans is warranted to further expand the potential impact of this tool. The automated segmentation failed in 16 cases (0.2%), largely due to an inability of the algorithm to determine the proper vertebral level. An exact determination into the specific causes of these failures has not yet been ascertained but could conceivably be due to CT artifact or noise, spinal hardware, or vertebral compression fractures, all of which could lead to segmentation error. Future work will focus on the source of computational errors in failed cases, with the hope of further improving the automated technique. Given the large cohort size, we did not review segmentation individually for each case. Lastly, this initial study did not attempt to correlate abdominal aortic calcium values with downstream adverse clinical outcomes. As mentioned, this critical next step will be the focus of future research. If we are successful in demonstrating clinical utility of this automated calcium tool in risk profiling, the next logical step would be widespread implementation as a prospective clinical tool.

In summary, we provide validation for a deep-learning-based automated aortic calcium segmentation tool at abdominal CT. This automated CT tool has the potential to provide both rapid and objective assessment and allowed us to apply it to a large retrospective research cohort and derive population-based normative values. We also found significant and interesting differences in Agatston score according to gender and age. By assessing the sub-cohort with longitudinal CT follow-up, this fully automated calcium segmentation method can also characterize interval changes in volume and mass over time. With further research, it may be possible to translate this information into an opportunistic approach to evaluate CVD risk on any routine abdominal CT, regardless of the study indication.

Acknowledgement This research was supported in part by the Intramural Research Program of the National Institutes of Health Clinical Center and made use of the high performance computing capabilities of the NIH Biowulf system.

Compliance with ethical standards

Conflict of interest The authors have no direct conflict of interest, but Dr. Pickhardt serves as an advisor to Bracco and is a shareholder in SHINE, Elucent, and Cellectar and Dr. Summers receives royalties from iCAD, PingAn, Philips and ScanMed and research support from PingAn and NVIDIA.

Ethical approval This study was approved by our institutional IRB.

References

1. Benjamin, E.J., et al., *Heart Disease and Stroke Statistics-2017 Update: A Report From the American Heart Association.* Circulation, 2017. **135**(10): p. e146-e603.
2. Sidney, S., et al., *Recent Trends in Cardiovascular Mortality in the United States and Public Health Goals.* JAMA Cardiol, 2016. **1**(5): p. 594-9
3. Hajar, R., *Framingham Contribution to Cardiovascular Disease.* Heart views: the official journal of the Gulf Heart Association, 2016. **17**(2): p. 78-81.
4. *Executive Summary of The Third Report of The National Cholesterol Education Program (NCEP) Expert Panel on Detection, Evaluation, And Treatment of High Blood Cholesterol In Adults (Adult Treatment Panel III).* Jama, 2001. **285**(19): p. 2486-97.
5. James, P.A., et al., *2014 evidence-based guideline for the management of high blood pressure in adults: report from the panel members appointed to the Eighth Joint National Committee (JNC 8).* Jama, 2014. **311**(5): p. 507-20.
6. Alqahtani, A.M., et al., *Quantifying Aortic Valve Calcification using Coronary Computed Tomography Angiography.* J Cardiovasc Comput Tomogr, 2017. **11**(2): p. 99-104.
7. Budoff, M.J., et al., *Thoracic aortic calcification and coronary heart disease events: the multi-ethnic study of atherosclerosis (MESA).* Atherosclerosis, 2011. **215**(1): p. 196-202.
8. DeLoach, S.S., et al., *Aortic calcification predicts cardiovascular events and all-cause mortality in renal transplantation.* Nephrology, dialysis, transplantation: official publication of the European Dialysis and Transplant Association - European Renal Association, 2009. **24**(4): p. 1314-1319.
9. O'Leary, D.H., et al., *Carotid-artery intima and media thickness as a risk factor for myocardial infarction and stroke in older adults. Cardiovascular Health Study Collaborative Research Group.* N Engl J Med, 1999. **340**(1): p. 14-22.
10. Pletcher, M.J., et al., *Using the coronary artery calcium score to predict coronary heart disease events: a systematic review and meta-analysis.* Arch Intern Med, 2004. **164**(12): p. 1285-92.
11. Eberhard, M., et al., *Quantification of aortic valve calcification on contrast-enhanced CT of patients prior to transcatheter aortic valve implantation.* EuroIntervention, 2017. **13**(8): p. 921-927.
12. Gernaat, S.A.M., et al., *Automatic quantification of calcifications in the coronary arteries and thoracic aorta on radiotherapy planning CT scans of Western and Asian breast cancer patients.* Radiother Oncol, 2018. **127**(3): p. 487-492.
13. Isgum, I., B. van Ginneken, and M. Olree, *Automatic detection of calcifications in the aorta from CT scans of the abdomen. 3D computer-aided diagnosis.* Acad Radiol, 2004. **11**(3): p. 247-57.
14. Zoghbi, W.A., *Cardiovascular imaging: a glimpse into the future.* Methodist DeBakey cardiovascular journal, 2014. **10**(3): p. 139-145.
15. Elmasri, K., et al., *Automatic Detection and Quantification of Abdominal Aortic Calcification in Dual Energy X-ray Absorptiometry.* Procedia Computer Science, 2016. **96**: p. 1011-1021.
16. Kurugol, S., et al., *Automated quantitative 3D analysis of aorta size, morphology, and mural calcification distributions.* Medical physics, 2015. **42**(9): p. 5467-5478.

17. O'Connor, S.D., et al., *Does Nonenhanced CT-based Quantification of Abdominal Aortic Calcification Outperform the Framingham Risk Score in Predicting Cardiovascular Events in Asymptomatic Adults?* Radiology, 2019. **290**(1): p. 108-115.
18. Pickhardt, P.J., *Imaging and Screening for Colorectal Cancer with CT Colonography.* Radiol Clin North Am, 2017. **55**(6): p. 1183-1196.
19. Chellamuthu, K., et al., *Atherosclerotic Vascular Calcification Detection and Segmentation on Low Dose Computed Tomography Scans Using Convolutional Neural Networks*, in *IEEE ISBI*. 2017: Melbourne, Australia. p. 388-391.
20. Liu, J., et al., *Pelvic artery calcification detection on CT scans using convolutional neural networks*, in *SPIE Medical Imaging*, S.G. Armato and N.A. Petrick, Editors. 2017. p. 101341A.
21. Liu, J., et al., *A Semi-Supervised CNN Learning Method with Pseudo-class Labels for Atherosclerotic Vascular Calcification Detection*, in *2019 IEEE 16th International Symposium on Biomedical Imaging (ISBI 2019)*, Venice, Italy, April 8-11, 2019. pp. 780-783.
22. Yao, J., O'Connor, S.D. and Summers, R.M. *Automated spinal column extraction and partitioning*. in *3rd IEEE International Symposium on Biomedical Imaging: Nano to Macro, 2006.* 2006.
23. He, K.M., et al., *Mask R-CNN.* 2017 Ieee International Conference on Computer Vision (Iccv), 2017: p. 2980-2988.
24. Rumberger, J.A. and L. Kaufman, *A Rosetta Stone for Coronary Calcium Risk Stratification: Agatston, Volume, and Mass Scores in 11,490 Individuals.* American Journal of Roentgenology, 2003. **181**(3): p. 743-748.
25. Dudina, A., et al., *Relationships between body mass index, cardiovascular mortality, and risk factors: a report from the SCORE investigators.* Eur J Cardiovasc Prev Rehabil, 2011. **18**(5): p. 731-42.
26. Khan, S.S., et al., *Association of Body Mass Index With Lifetime Risk of Cardiovascular Disease and Compression of Morbidity.* JAMA Cardiol, 2018. **3**(4): p. 280-287.
27. Mancio, J., et al., *Association of body mass index and visceral fat with aortic valve calcification and mortality after transcatheter aortic valve replacement: the obesity paradox in severe aortic stenosis.* Diabetol Metab Syndr, 2017. **9**: p. 86.
28. Glodny, B., et al., *A method for calcium quantification by means of CT coronary angiography using 64-multidetector CT: very high correlation with Agatston and volume scores.* Eur Radiol, 2009. **19**(7): p. 1661-8.
29. Laudon, D.A., et al., *Computed tomographic coronary artery calcium assessment for evaluating chest pain in the emergency department: long-term outcome of a prospective blind study.* Mayo Clinic proceedings, 2010. **85**(4): p. 314-322.
30. Li, Q., et al., *Coronary artery calcium quantification using contrast-enhanced dual-energy computed tomography scans in comparison with unenhanced single-energy scans.* Phys Med Biol, 2018. **63**(17): p. 175006.
31. Moreno, C.C., et al., *Changing Abdominal Imaging Utilization Patterns: Perspectives From Medicare Beneficiaries Over Two Decades.* Journal of the American College of Radiology, 2016. **13**(8): p. 894-903.
32. Lee, S.J. and P.J. Pickhardt, *Opportunistic Screening for Osteoporosis Using Body CT Scans Obtained for Other Indications: the UW Experience.* Clinical Reviews in Bone and Mineral Metabolism, 2017. **15**(3): p. 128-137.
33. Pickhardt, P.J., et al., *Opportunistic Screening for Osteoporosis Using Abdominal Computed Tomography Scans Obtained for Other Indications.* Annals of Internal Medicine, 2013. **158**(8): p. 588-595.
34. Boyce, C.J., et al., *Hepatic Steatosis (Fatty Liver Disease) in Asymptomatic Adults Identified by Unenhanced Low-Dose CT.* American Journal of Roentgenology, 2010. **194**(3): p. 623-628.
35. Pickhardt, P.J., et al., *Natural History of Hepatic Steatosis: Observed Outcomes for Subsequent Liver and Cardiovascular Complications.* American Journal of Roentgenology, 2014. **202**(4): p. 752-758.
36. Pickhardt, P.J., et al., *Visceral Adiposity and Hepatic Steatosis at Abdominal CT: Association With the Metabolic Syndrome.* American Journal of Roentgenology, 2012. **198**(5): p. 1100-1107.
37. Pickhardt, P.J., et al., *CT colonography to screen for colorectal cancer and aortic aneurysm in the Medicare population: cost-effectiveness analysis.* AJR Am J Roentgenol, 2009. **192**(5): p. 1332-40.
38. Lee, S.J., et al., *Fully automated segmentation and quantification of visceral and subcutaneous fat at abdominal CT: application to a longitudinal adult screening cohort.* Br J Radiol, 2018. **91**(1089): p. 20170968.
39. Lee, S.J., P.A. Anderson, and P.J. Pickhardt, *Predicting Future Hip Fractures on Routine Abdominal CT Using Opportunistic Osteoporosis Screening Measures: A Matched Case-Control Study.* AJR Am J Roentgenol, 2017. **209**(2): p. 395-402.
40. Lee, S.J., et al., *Future Osteoporotic Fracture Risk Related to Lumbar Vertebral Trabecular Attenuation Measured at Routine Body CT.* J Bone Miner Res, 2018. **33**(5): p. 860-867.
41. Pickhardt, P.J., et al., *Population-based opportunistic osteoporosis screening: Validation of a fully automated CT tool for assessing longitudinal BMD changes.* British Journal of Radiology, 2019. **92**(1094).